



THREE FRAGMENT FISSION IN ACTINIUM NUCLEI

A.V.Mahesh Babu¹, N. Sowmya^{*2}, H.C. Manjunatha², P.S. Damodara Gupta²¹Department of Physics, Smt Danamma Channabasavai college of Arts, Science, Commerce & Management Studies, Kolar, Karnataka, India²Department of Physics, Government College for Women, Kolar, Karnataka, India^{*}Corresponding author: sowmyaprakash8@gmail.com

ABSTRACT

The most possible alpha-accompanied ternary fission fragment of $^{217-219}\text{Ac}$ are studied using Coulomb and proximity potential model. We have studied driving potential (V-Q), logarithmic half-lives and relative yield of all possible fission fragments. From the present work, the minimum driving potential, maximum relative yield and minimum half-lives are observed for the fragment combination of $^4\text{He}+^{209-211}\text{Ac}+^4\text{He}$ for the nuclei $^{217-219}\text{Ac}$. Hence, this fission fragment combination is considered as most possible fission fragments due to presence of doubly magic nuclei. This study is important in near future experiments.

Keywords: Half-lives, Ternary fission, Driving potential, Relative yield.

1. INTRODUCTION

Ternary fission is the splitting of a heavy radioactive nucleus into three fission fragments. The light particle emitted is almost perpendicular to fission axis. These light ternary particle is emitted from the neck region and accelerated by the Coulomb field of other two heavier fragments. Many theoretical models such as Coulomb and Proximity potential model [1] were successful in explaining the possible fission yield in the ternary fission. By taking nuclear proximity effects in liquid drop model Royer et al., [2] investigated prolate and oblate ternary fission and cascade fission in ^{56}Fe , ^{149}Eu , ^{240}Pu and also in ^{298}Fl . The total energy released during ternary fission is larger when compared to binary fission[3]. Using Coulomb and proximity potential model the possible ternary fission fragments were identified in the superheavy region [4-12]. Previous researchers have used modified generalised liquid drop model, Coulomb and proximity potential model and effective liquid drop model were used to study alpha-decay and cluster decay.

The energy necessary to generate ternary fission particles is provided by the rapid collapse of the neck into the fission fragments after scission [19]. Raisbeck [20] experimentally measured ternary fission of ^{252}Cf by angular distributions and energy spectrum of light particle emissions such as $^1,2,3\text{H}$, $^{4,6,8}\text{He}$, Li and Be. The

traces of light charged particles such as H, He, Li and Be were observed in ternary fission of ^{252}Cf [21-22]. In light charged particle-accompanied ternary fission the total kinetic energy corresponding to fragments is close to its ternary decay energy (Q-value) [23]. Ternary fission of actinide nuclei ^{252}Cf shows third fragment heavier than ^{14}C in spontaneous ternary fission. Karthik and Balasubramaniam studied binary and ternary fission of ^{235}U using modified scission point model [24]. Although no thorough study has been done into ternary mass distribution, experimental and theoretical investigations have shown the likelihood of ternary emission of various radioactive nuclei such as ^{235}U , ^{252}Cf and ^{241}Pu induced and spontaneous fission in thermal neutron [25-36].

Through literature survey shows α -accompanied ternary fission in U, Pu and Cf. Hence, in the present work, we have studied α -accompanied ternary fission in $^{217-219}\text{Ac}$ using Coulomb and proximity potential model. Since, the half-lives corresponding to these nuclei are in nanoseconds to micro seconds which are highly unstable. Hence, we made an effort to predict possible fission fragments in these nuclei. The driving-potential (V-Q), probability of fission and yield for each individual fragments were carried out and identified possible ternary fission fragments. The present work is organised as follows; theory used to study α -

accompanied ternary fission in Actinium nuclei ($^{217-219}\text{Ac}$) is presented in Sec 2. Results and discussions were shown in Sec 3. Conclusions drawn from the present work is in Sec 4.

2. THEORY

Ternary fission followed by light charged particle emission is energetically feasible if the Q value of the reaction is positive.

$$Q = M - \sum_{i=1}^3 m_i > 0 \quad (1)$$

Here M and m_i are the mass excess of the parent and mass excess of the fission fragments respectively. Interacting potential barrier exhibiting ternary fission consists of Coulomb and proximity potential.

$$V = \sum_i \sum_{j>i}^3 (V_{cij} + V_{rij}) \quad (2)$$

Here V_{cij} is due to Coulomb interaction between the fragments and it is given as

$$V_{cij} = \frac{Z_i Z_j e^2}{r_{ij}} \quad (3)$$

Here Z_i , Z_j and r_{ij} are the atomic numbers of the fragments and distance between fragment centres. The nuclear proximity potentials is given by

$$V_p(Z) = 4\pi\gamma\bar{R}\Phi\left(\frac{z}{b}\right) \quad (4)$$

Here Φ and z are the universal proximity potential and distance between the near surfaces of the fragments respectively. $b \approx 0.99$ is the nuclear surface thickness. Where, $z_{12} = z_{23} = z_{13} = z$ are the distance between the near surfaces of the fission fragments. For this proximity potential the universal function is given [37]

$$\Phi(S_0) = \begin{cases} \Phi(S_0) = \left\{ \left(-\frac{1}{2} \right) (S_0 - 2.54)^3 - 0.0852 (S_0 - 2.54)^3 \right\} & \text{for } S_0 < 1.2511 \\ -3.437 \exp\left(-\frac{S_0}{0.75}\right) & \text{for } S_0 > 1.2511 \end{cases} \quad (5)$$

The surface energy constant γ [38] in equation (4)

$$\gamma = \gamma_0 \left[1 - k_s \left(\frac{N - Z}{A} \right)^2 \right] \quad (6)$$

Here N and Z are the neutrons and proton number respectively. The coefficients γ_0 and k_s are 0.9517 MeV/fm² and 1.7826, respectively. The mean curvature radius \bar{R} , Sussmann central radii C_i and sharp radii R_i is explained in reference [11]. The logarithmic half-lives and relative yield is evaluated as explained in reference [11].

3. RESULTS AND DISCUSSION

The amount of energy released during an alpha accompanied ternary fission is evaluated using recent mass excess values [39]. The total potential, penetration probability using WKB integral, logarithmic half-lives and relative yield is evaluated as explained in the theory section for the nuclei $^{217-219}\text{Ac}$. The structure of driving potential is evaluated using the concept of reaction valley. The minimum driving potential ($V-Q$) is evaluated using Coulomb and proximity potential model. The mass excess of each fragment combination is extracted such that the $Q > 0$. For the alpha accompanied ternary fission of nuclei $^{217-219}\text{Ac}$ by fixing A_3 to ^4He . The driving potential for all possible fission fragments of A_1 and A_2 are evaluated in the equatorial configuration. The values of A_1 increases from 2 to 106 and the value of A_2 decreases from 211 to 107 in case of ^{217}Ac .

Similarly, A_1 and A_2 range between 2-108 and 213-107 respectively. The Fig.-1(a-c) shows the studied driving potential with respect to fission fragment mass number A_1 . From the Fig.1(a) it has been observed that the minimum driving potential is observed for the fission fragment combination such as $^4\text{He} + ^{209}\text{Ac}$, $^8\text{Be} + ^{205}\text{Bi}$, $^{12}\text{C} + ^{201}\text{Tl}$, $^{36}\text{S} + ^{177}\text{Lu}$, $^{50}\text{Ti} + ^{163}\text{Tb}$, $^{70}\text{Zn} + ^{143}\text{La}$, $^{84}\text{Kr} + ^{129}\text{Sb}$ and $^{102}\text{Ru} + ^{111}\text{Tc}$ by keeping third fission fragment ^4He as constant. In all these cases in which driving potential observed minimum is consisting of either magic or semi-magic nuclei as a first and second fission fragment. In case of fission fragment combination of $^4\text{He} + ^{209}\text{Ac}$, ^4He is having magic number with $Z=2$ shows extra stability against their neighbouring nuclei. Similarly, ^{70}Zn is as a semi-magic nuclei and other fission fragments are near magic or semi-magic nuclei which are stable when compared to their neighbouring ones. In case of nuclei ^{218}Ac and ^{219}Ac shows minimum driving potentials in case of $^4\text{He} + ^{209-210}\text{Ac}$, $^8\text{Be} + ^{205-206}\text{Bi}$, $^{12}\text{C} + ^{201-202}\text{Tl}$, $^{36}\text{S} + ^{177-178}\text{Lu}$, $^{50}\text{Ti} + ^{163-164}\text{Tb}$, $^{70}\text{Zn} + ^{143-125}\text{La}$, $^{84}\text{Kr} + ^{129-130}\text{Sb}$ and $^{102}\text{Ru} + ^{111-112}\text{Tc}$ respectively and it is depicted in Fig. 1(b) and 1(c).

The Fig. 2(a-c) shows the studied alpha-accompanied ternary fission for the nuclei $^{217-219}\text{Ac}$. From the Fig. 2(a) it is clear that the fission fragment combination $^4\text{He} + ^{209}\text{Ac}$, $^8\text{Be} + ^{205}\text{Bi}$, $^{12}\text{C} + ^{201}\text{Tl}$, $^{36}\text{S} + ^{177}\text{Lu}$, $^{50}\text{Ti} + ^{163}\text{Tb}$, $^{70}\text{Zn} + ^{143}\text{La}$, $^{84}\text{Kr} + ^{129}\text{Sb}$ and $^{102}\text{Ru} + ^{111}\text{Tc}$ shows shorter half-lives when compared to other fission fragment combinations studied. Among all these fission fragment combination, the combination $^4\text{He} + ^{209}\text{Ac} + ^4\text{He}$ is having shorter logarithmic half-lives when compared to their neighbouring nuclei. Hence, the most possible fission fragment combination is $^4\text{He} + ^{209}\text{Ac} + ^4\text{He}$ in

case of nuclei ^{217}Ac . Furthermore, the nuclei ^{218}Ac and ^{219}Ac also shows shorter half-lives for the fission

fragments $^4\text{He}+^{210}\text{Ac}+^4\text{He}$ and $^4\text{He}+^{211}\text{Ac}+^4\text{He}$ respectively.

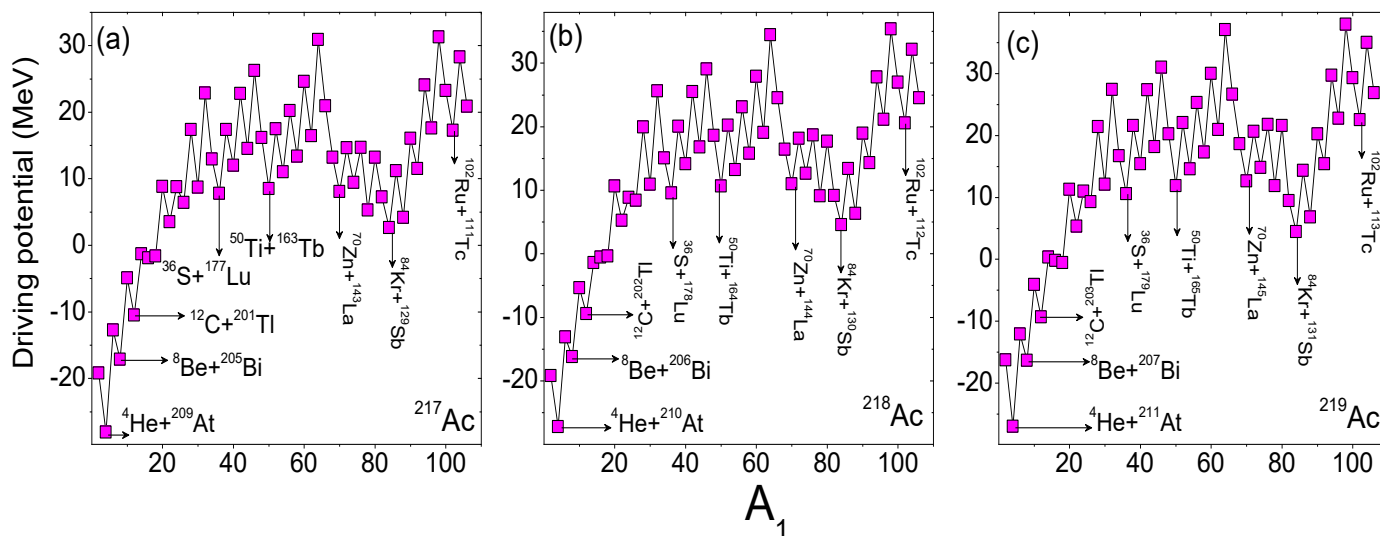


Fig. 1: Variation of driving potential with the fission fragment mass number A_1 for alpha accompanied ternary fission of $^{217-219}\text{Ac}$.

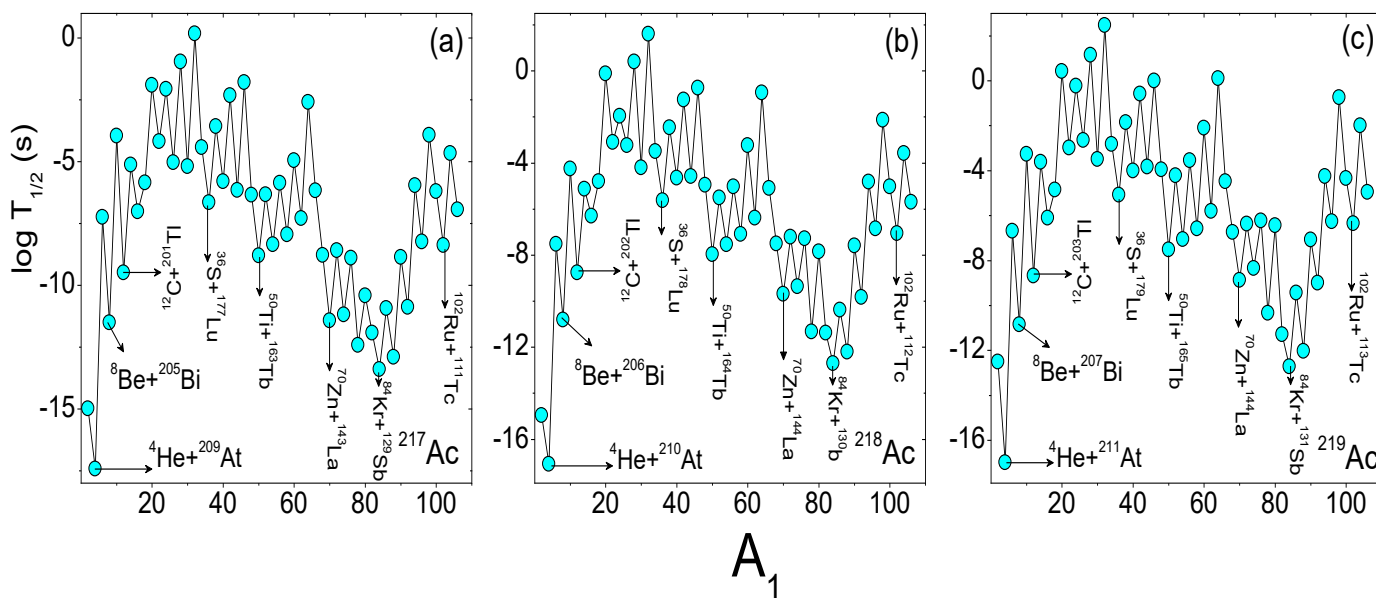


Fig. 2: Calculated logarithmic half-lives of alpha accompanied ternary fission with the mass number of fission fragment A_1 for the nuclei $^{217-219}\text{Ac}$

The evaluated relative yield for alpha accompanied ternary fission of $^{217-219}\text{Ac}$ as function of mass number of A_1 is shown in Fig. 3(a-c). From the Fig. 3(a) it is clear that, the maximum relative yield corresponding to $^4\text{He}+^{209}\text{Ac}+^4\text{He}$ shows larger value when compared to their neighbouring fission fragments studied. Furthermore, the nuclei ^{218}Ac and ^{219}Ac shows larger relative yield for the fission fragments $^4\text{He}+^{210}\text{Ac}+^4\text{He}$

and $^4\text{He}+^{211}\text{Ac}+^4\text{He}$ respectively. Hence, the detail study shows that the minimum driving potential, larger relative yield and shorter logarithmic half-lives corresponding $^4\text{He}+^{209}\text{Ac}+^4\text{He}$, $^4\text{He}+^{210}\text{Ac}+^4\text{He}$ and $^4\text{He}+^{211}\text{Ac}+^4\text{He}$ in case of nuclei $^{217-219}\text{Ac}$ are considered as most possible fission fragments with doubly magic nucleus ^4He ($Z=2$, $N=2$).

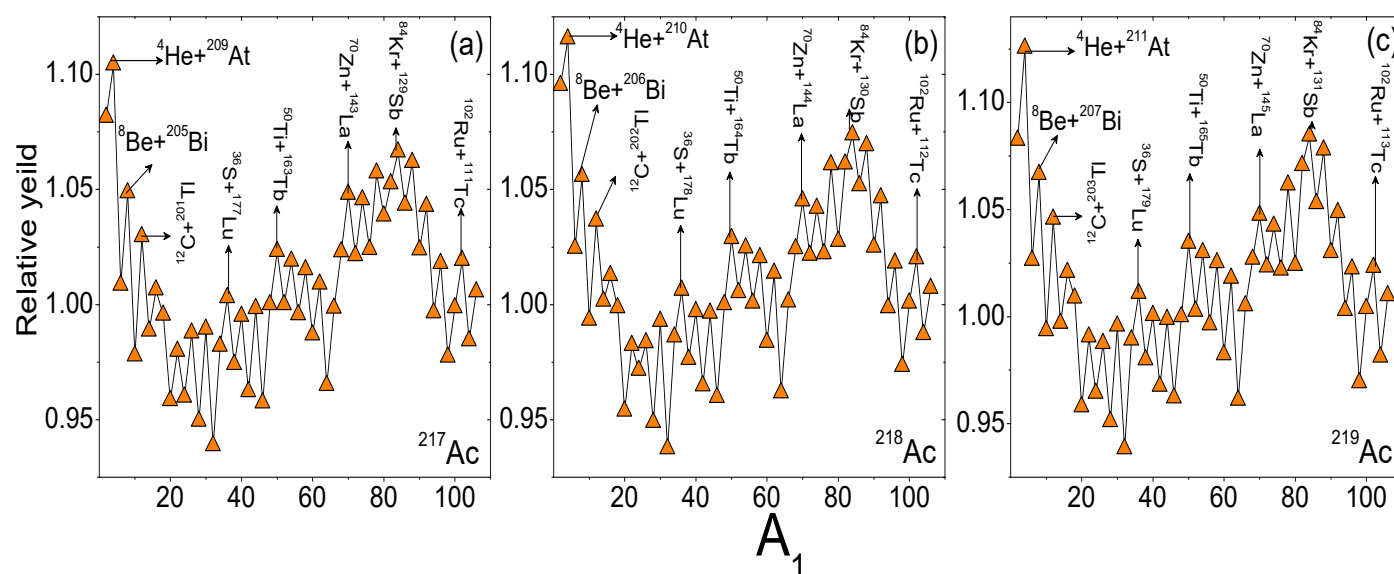


Fig. 3: Plot of relative yield for the alpha accompanied ternary fission of $^{217-219}\text{Ac}$ with mass number of fission fragment A_1

4. CONCLUSION

An alpha accompanied ternary fission is studied using Coulomb and proximity potential model in equatorial configuration. The amount of energy released during ternary fission is evaluated using recent mass excess data. Driving potential, logarithmic half-lives and relative yield are evaluated. From the present study it is clear that the fission fragment combination $^4\text{He}+^{209}\text{Ac}+^4\text{He}$, $^4\text{He}+^{210}\text{Ac}+^4\text{He}$ and $^4\text{He}+^{211}\text{Ac}+^4\text{He}$ possess minimum driving potential, larger relative yield and shorter half-lives for the nuclei $^{217-219}\text{Ac}$ due to the existence of doubly magic nuclei ^4He ($Z=2$, $N=2$). Hence, ^4He and $^{209-211}\text{Ac}$ are most possible alpha ternary fission fragments in $^{217-219}\text{Ac}$ nuclei.

5. REFERENCES

- Bunakov VE, Kadmensky SG. *Phys. Atom. Nuclei*, 2003; **66**:1846-1860.
- Royer G, Haddad F, Mignen J. *J. Phys. G: Nucl. Part. Phys.*, 1992; **18**:2015-2026.
- Swiatecki W J. *Second UN Int. Conf. on the Peaceful Uses of Atomic Energy*, Geneva, 1958; 651.
- Manjunatha HC, Sowmya N. *Nucl. Phys. A*, 2018; **969**:68-82.
- Manjunatha HC, Sowmya N. *International Journal of Modern Physics E*, 2018; **27(5)**:1-17.
- Manjunatha HC, Sridhar K N, Sowmya N. *Phys. Rev. C*, 2018; **98**:024308.
- Sowmya N, Manjunatha HC. *Bulg. J. Phys.*, 2019; **46**:16-27.
- Zagrebaev VI, Karpov AV. Walter Greiner. *Phys. Rev. C*, 2010; **81**:1-5.
- Vijayaraghavan K R, Balasubramaniam M, von Oertzen W. *Phys. Rev. C*, 2015; **91**:1-4.
- Diehl H, Greiner W. *Nuclear Physics A*, 1974; **229(1)**:29-46.
- Manjunatha HC, Sowmya N, Sridhar KN, Seenappa L. *Jour. of Rad. Nucl.chem.*, 2017; **314(2)**: 991-999.
- Sowmya N, Manjunatha HC, Dhananjaya N. *Jour. Radi. Nuc.chem*, 2020; **323**:1347-1351.
- Sowmya N and Manjunatha H C. *Braz J Phys*, 2019; **49**:874.
- Sowmya N, Manjunatha HC. *Braz Jour of Phys*, 2020; **50**:317.
- Srinivas MG, Manjunatha HC, Sridhar KN, Sowmya N, Raj AC. *Nucl Phys A*, 2020; **995**: 1216.
- Sridhar GR, Manjunatha HC, Sowmya N, Gupta P S D, Ramalingam H B. *Eur. Phys. J. Plus*, 2020; **135**:291.
- Sowmya N, Manjunatha HC. *Phys of Part and Nuclei Lett*, 2020; **17(3)**:370.
- N Sowmya N, Manjunatha HC. *J. Phys. G. Nucl. Part. Phys*, 2010; **37**:1-14
- Halpern I. *In Proceedings of the IAEA Symposium on the Physics and Chemistry of Fission, Salzburg*, 1965; **Vol. 2** (International Atomic Energy Agency, Vienna, 1965); p. 369.
- Raisbeck GM, Thomas TD. *Phys. Rev*, 1968; **172**:1272.

21. Whetstone SL, Thomas TD. *Phys. Rev. Lett.*, 1965; **15**:298.
22. Whetstone SL, Thomas TD. *Phys. Rev.*, 1967; **154**:1174.
23. Manimaran K, Balasubramaniam M. *Eur. Phys. J.*, 2010; **A 45**:293-300.
24. Karthika C, Balasubramaniam M. *Eur. Phys. J. A*, 2019; **55(59)**:1-10.
25. Fong P. *Phys. Rev. C*, 1971; **3**:2025-2027.
26. Diehl H, Greiner W. *Nucl. Phys.A*, 1974; **229**:29-46.
27. Rubchenya V A, Yavshits S G. *Z. Phys.A-Atom. Nucl.*, 1988; **329**:217-228.
28. Sandulescu A, Crstoiu F, Misicu S, Florescu A, Ramayya AV. Hamilton JH, et al. *J. Phys. G*, 1998; *Nucl. Part. Phys.* **24**:181.
29. Poenaru D N, Greiner W, Gherghescu R. *Atomic Data and Nuclear data Tables*, 1998; **68**:91-147.
30. Koster U, Faust H, Fioni G, Friedrichs T, Gro M, Oberstedt S. *Nuclear Physics A*, 1999; **652**:371-387.
31. Sandulescu A, Carstoiu F, Bulboacă I, Greiner W. *Phys. Rev C*, 1999; **60**:1-13.
32. Poenaru DN, Dobrescu B, Greiner W, Hamilton J H, Ramayya AV. *Jour Phys G:Nucl.par. phys*, 2000; **6**: L97-L102.
33. Lestone JP. *Phys. Rev. C*, 2004; **70**:1-5.
34. Gherghescu RA, Poenaru DN, Greiner W. *Int. J. Mod.Phys.*, 2008; **E1**:2221.
35. Manimaran K, Balasubramaniam M. *Phys. Rev. C*, 2009; **79**:1-8.
36. Manimaran K, Balasubramaniam M. *J. Phys. G Nucl. Part. Phys*, 2010; **37**:1-14.
37. Naumann RA, Inorg J. *Nucl. Chem.*, 1960; **16(1)**: 163-164.
38. Myers WD, Swiatecki W J. *Annal. Phys*, 1974; **84(1-2)**:186-210.
39. Meng Wang et al., *Chinese Phys.C*, 2021;**45**:030003.